

parameters, number of layers, and imaging conditions. Molecular layers attached to a layer below by a tailgroup-tailgroup interface were disordered and much more weakly bound. Monolayers attached by headgroup binding to a substrate formed a disordered and relatively unstable film. This result is intriguing and quite surprising, considering that the specific lattice structure that we measure is determined by the close packing of the alkane chains. However, we speculate that, in the LB geometry, the electrostatic interaction between headgroups and divalent cations is necessary to stabilize a long-range structure. These observations are confirmed by electron (3–5) and x-ray (7) diffraction results which show that the translational correlation length in monolayers is between 30 and 100 Å, significantly less than the ≥ 350 Å we have seen on the thicker films. The importance of the headgroup-headgroup interface may explain the well-known empirical result that LB films of fatty acid salts (with divalent cations) are more stable (13) and easier to make (27) than LB films of the analogous fatty acid. It is also likely that the strong headgroup interaction is the energetic driving force of the reorganization under water.

In order to confirm our AFM studies, electron diffraction studies were done on 1- and 3-layer films on a hydrophilic substrate. The diffraction pattern from the 3-layer film agreed both in symmetry and lattice parameters with our AFM results. The diffraction from the monolayer agrees with other electron and x-ray diffraction data (2–4, 7) and shows a hexagonal structure with a nearest-neighbor distance of 0.47 ± 0.01 nm, giving an area per molecule of 19.4 \AA^2 , $\sim 8\%$ larger than in multilayer films. The extra area per molecule of the monolayer film and the short-range positional correlation length (3–5, 7) implies that there is considerable motion and disorder within the individual alkane chains as compared to the close-packed chains in the multilayer (area per molecule of 18 \AA^2). This interpretation is supported by FTIR spectroscopy (2, 16), which shows that the alkane chains of monolayers show less crystallinity than do thicker films. This result corroborates our claim that our inability to image a lattice structure on monolayers in air and bilayers under water implies that they are inherently disordered.

The AFM images show that the essential factor in determining order and stability in the alkyl chains in cadmium arachidate films is the presence of an adjacent headgroup-headgroup interface stabilized by cadmium ions. The role of an interface (substrate or free surface) in determining molecular ordering is only to allow or disallow the adjacent headgroup-headgroup stabilization. The structure and phase of the monolayer on the

subphase are also not simply related to the structure and phase of the deposited LB film; strong coupling effects to other layers have an equal or greater effect on determining the structure of the deposited films.

REFERENCES AND NOTES

- G. G. Roberts, *Adv. Phys.* **34**, 475 (1985).
- A. Bonnerot, P. A. Chollet, H. Frisby, M. Hoclet, *J. Chem. Phys.* **97**, 365 (1985).
- S. Garoff, H. W. Deckman, J. H. Dunsmuir, M. S. Alvarez, *J. Phys. (France)* **47**, 701 (1986).
- C. Böhm, R. Seitz, H. Riegler, *Thin Solid Films* **178**, 511 (1989).
- I. R. Peterson, R. Seitz, H. Krug, I. Voigt-Martin, *J. Phys. (France)* **51**, 1003 (1990).
- M. Seul, P. Eisenberger, H. M. McConnell, *Proc. Natl. Acad. Sci. U.S.A.* **80**, 5795 (1983); M. Prakash, P. Dutta, J. B. Ketterson, B. M. Abraham, *Chem. Phys. Lett.* **111**, 395 (1984).
- P. Tippmann-Krayer, R. M. Kenn, H. Möhwald, *Thin Solid Films* **210**, 577 (1992).
- M. Pomerantz and A. Segmüller, *ibid.* **68**, 33 (1980).
- R. F. Fischetti, V. Skita, A. F. Garito, J. K. Blasie, *Phys. Rev. B* **37**, 4788 (1988); S. Xu, A. Murphy, S. M. Amador, J. K. Blasie, *J. Phys. I (France)* **1**, 1131 (1991).
- V. Skita, W. Richardson, M. Filipkowski, A. Garito, J. K. Blasie, *J. Phys. (France)* **47**, 1849 (1986); V. Skita, M. Filipkowski, A. F. Garito, J. K. Blasie, *Phys. Rev. B* **34**, 5826 (1986).
- J. M. Bloch, W. B. Yun, K. M. Mohanty, *Phys. Rev. B* **40**, 6529 (1989).
- D. A. Outka, J. Stöhr, J. P. Rabe, J. D. Swalen, H. Rotermund, *Phys. Rev. Lett.* **59**, 1321 (1987).
- P. M. Claesson and J. M. Berg, *Thin Solid Films* **176**, 157 (1989).
- L. Rothberg, G. S. Higashi, D. L. Allara, S. Garoff, *Chem. Phys. Lett.* **133**, 67 (1987); J. P. Rabe, J. D. Swalen, J. F. Rabolt, *J. Chem. Phys.* **86**, 1601 (1987); T. Nakanaga, M. Matsumoto, Y. Kawabata, H. Takeo, C. Matsamura, *Chem. Phys. Lett.* **160**, 129 (1989).
- P. Stroeve, M. P. Srinivasan, B. G. Higgins, S. T. Kowel, *Thin Solid Films* **146**, 209 (1987).
- R. Maoz and J. Sagiv, *J. Colloid Interface Sci.* **100**, 465 (1984); F. Kimura, J. Umemura, T. Takekura, *Langmuir* **2**, 96 (1986).
- L. Bourdieu, P. Silberzan, D. Chatenay, *Phys. Rev. Lett.* **67**, 2029 (1991); E. Meyer *et al.*, *Nature* **349**, 398 (1991); J. A. N. Zasadzinski *et al.*, *Biophys. J.* **59**, 755 (1991).
- J. K. H. Hörber, C. A. Lang, T. W. Hänsch, W. M. Heckl, H. Möhwald, *Chem. Phys. Lett.* **145**, 151 (1988).
- J. Garnaes, D. K. Schwartz, R. Viswanathan, J. A. N. Zasadzinski, *Nature* **357**, 54 (1992).
- Materials: arachidic acid (Aldrich, 99%), chloroform (Fisher spectranalyzed), water (Milli-Q, Millipore, Bedford, MA), CdCl_2 (Aldrich, 99.99%), and NaHCO_3 (Aldrich, 99.95%).
- Silicon wafers polished on both sides [orientation (100), 3 to 5 ohm-cm, *n*-type, ~ 0.4 mm thick] with a root-mean-square roughness of ~ 2 Å as measured by AFM (Semiconductor Processing, Boston, MA).
- NIMA Technology, Warwick Science Park, Coventry, CV4 7EZ United Kingdom.
- Nanoscope II FM, Digital Instruments, Goleta, CA 93117.
- A. I. Kitaigorodskii, *Organic Chemical Crystallography* (Consultants Bureau, New York, 1961); F. Leveiller *et al.*, *Science* **252**, 1532 (1991); M. L. Schlossman *et al.*, *Phys. Rev. Lett.* **66**, 1599 (1991).
- R. Steitz, E. E. Mitchell, I. R. Peterson, *Thin Solid Films* **205**, 124 (1991).
- J. N. Israelachvili, *Intermolecular and Surface Forces* (Academic Press, London, ed. 2, 1992), chap. 15.
- E. P. Honig, J. H. Th. Hengst, D. den Engelsen, *J. Colloid Interface Sci.* **45**, 92 (1973).
- D. K. Schwartz, J. Garnaes, R. Viswanathan, S. Chiruvolu, J. A. N. Zasadzinski, *Phys. Rev. A*, in press.
- Supported by the Office of Naval Research under grant N00014-90-J-1551, the National Science Foundation under grant CTS90-15537, and the Donors of the Petroleum Research Foundation. We acknowledge S. Chiruvolu for the TED experiments and J. Israelachvili, W. Ducker, and S. Steinberg for useful discussions. We also thank F. Grunfeld of NIMA Technologies for his assistance with the trough and software. J.G. acknowledges support from the Danish Technical Research Council.

1 April 1992; accepted 29 May 1992

Existence of an Orientational Electric Dipolar Response in C_{60} Single Crystals

G. B. Alers, Brage Golding,* A. R. Kortan, R. C. Haddon, F. A. Theil

The dielectric constant ϵ and conductivity σ of undoped C_{60} single crystals have been measured as a function of temperature, $10 \text{ K} < T < 330 \text{ K}$, and frequency, $0.2 \text{ kilohertz} < f < 100 \text{ kilohertz}$. On cooling below the first-order structural phase transition at 260 K, a Debye-like relaxational contribution to the dielectric response is observed, which requires the presence of permanent electric dipoles. The relaxation rate is thermally activated with a broad distribution of energies centered at 270 millielectron volts. The existence of a dipole moment in C_{60} is unexpected, because it is precluded by symmetry for the pure ordered cubic phase. These data suggest that the high degree of frozen-in orientational disorder of the C_{60} molecules is responsible for the existence of electric dipolar activity.

The discovery and synthesis of the icosahedral carbon molecule C_{60} (1) and its subsequent crystallization (2) have stimulated great activity directed toward understanding the static and dynamic properties of its solid phases. At room temperature,

C_{60} forms a face-centered cubic (fcc) crystal (3) that is stabilized primarily by intermolecular van der Waals interactions (4, 5). Each C_{60} molecule undergoes nearly free rotation at its lattice site (6–8) and can be considered to have time-averaged spherical

symmetry. Near 260 K, a first-order phase transition occurs in which each C_{60} molecule acquires a net orientation along specific crystallographic directions, forming four interpenetrating simple cubic (sc) sublattices (3, 9). Nevertheless, orientational hopping can still occur, as was initially inferred from nuclear magnetic resonance spectroscopy (NMR) (6, 8) and by sound attenuation (10) experiments. As the temperature decreases, the orientational fluctuations become comparable to, or longer than, measurement time scales. Recently, evidence for a relatively large amount of frozen-in disorder below 100 K has been reported (11). Such disorder is important for it may influence such crystal properties as low-temperature thermal conductivity (12) and specific heat (13), as well as fundamental electronic properties such as electronic transport or optical response (14). Furthermore, the slow orientational dynamics of C_{60} at low temperatures has raised the possibility of a transition into a glassy phase (4, 11).

We present results for the low-frequency dielectric response of nominally pure single crystals of cubic C_{60} . We find that both the dielectric permittivity $\epsilon(\omega, T)$ and the conductivity $\sigma(\omega, T)$ exhibit temperature-dependent structure below 300 K. Well below $T_c = 260$ K, where the structural phase transition from fcc to sc occurs, we observe a frequency-dependent contribution to ϵ and σ that requires the presence of permanent electric dipoles. The dynamics of the dipoles correspond to thermally activated rotational motion of the C_{60} over a potential barrier $E_0 = 270$ meV. We find evidence of appreciable structural disorder as manifested in a distribution of activation energies with a width about 20% of E_0 . We suggest that orientational disorder can account for the observed electric dipole moment that would otherwise not be allowed in the centrosymmetric structure of cubic C_{60} .

Measurements were performed on two single crystal samples, S_1 and S_2 , grown by vapor transport in high vacuum from high-purity powder (15). Sample S_1 had linear dimensions of approximately 0.2 mm on all sides, whereas S_2 had dimensions 0.2 by 0.3 by 0.5 mm³. The crystals were naturally faceted platelets with predominantly (111) faces. Gold films were evaporated onto parallel faces of the crystals to form capacitors $\approx 10^{-2}$ pF. The samples were mounted in a three-terminal configuration such that stray capacitances were reduced to less than

10^{-3} pF and attached to minimize thermally induced stresses. A capacitance bridge and lock-in amplifier were used to obtain ϵ and σ over the frequency range 0.2 to 100 kHz. Sensitivity to relative changes in ϵ was better than 10^{-4} . The absolute capacitance was consistent with a static dielectric constant of 4.4, as reported for films (16). Response was linear for all electric fields used, which were less than 500 V cm⁻¹. Both samples yielded identical results for the temperature dependence of $\epsilon(\omega, T)$ but differed substantially in values of σ . The room-temperature conductivity at 1 kHz of S_1 is $\sigma = 2 \times 10^{-10}$ (ohm-cm)⁻¹ whereas for S_2 $\sigma = 1 \times 10^{-9}$ (ohm-cm)⁻¹. The temperature dependence of the conductivity in the region 260 K < T < 320 K is thermally activated and was fit to a function of the form $\exp(-E_g/2k_B T)$ with $E_g = 1.6 \pm 0.3$ eV for S_1 and 1.4 ± 0.3 eV for S_2 (k_B is the Boltzmann constant). Previous conductivity measurements in C_{60} powders at high pressures found a gap of 1.6 ± 0.1 eV in what is presumed to be the fcc phase (17). These results are consistent with electronic structure calculations that yielded a semiconductor gap $E_g = 1.3$ to 1.5 eV (18).

Figure 1 shows $\Delta\epsilon/\epsilon$ and σ at 10 kHz for temperatures between 75 and 275 K with evidence of structure at 260 and 165 K. The dielectric response for the temperature range 10 K < T < 75 K was featureless within our resolution. At 260 K a discontinuous increase in both σ and $\Delta\epsilon/\epsilon$ occurs upon cooling, which we associate with the fcc-sc structural phase transition. At this temperature the C_{60} dynamics change from

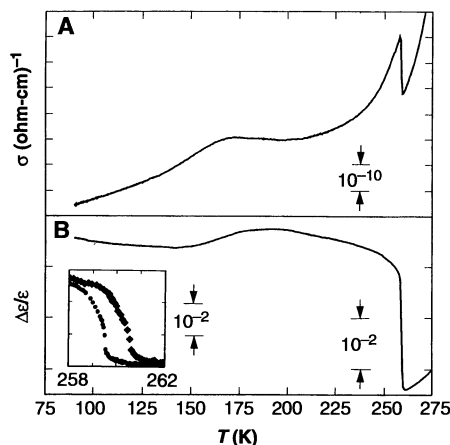


Fig. 1. Dielectric permittivity change $\Delta\epsilon/\epsilon$ (B) and conductivity σ (A) for the dielectric response of single crystal C_{60} at 10 kHz. Dipolar relaxation produces a knee in $\Delta\epsilon/\epsilon$ and a peak in σ near 165 K at this frequency. Discontinuities occur in both components of the dielectric response at the 260 K phase transition. The inset shows an expanded view of the transition region demonstrating the thermal hysteresis exhibited on cooling (●) and heating (◆). The rate of cooling or heating was less than 10^{-2} K s⁻¹.

essentially free rotation about arbitrary axes (6, 7) to an orientationally ordered phase with fluctuations characterized by discrete jumps over an energy barrier (6, 8). The abrupt change in the dielectric function at the phase transition indicates the sensitivity of this electronic property to the orientational order of the crystal. The inset in Fig. 1 shows a thermal hysteresis with a width of ~ 1 K, illustrating that the transition is first order (11, 19). The width was independent of heating or cooling rates for the range 10^{-1} K s⁻¹ < dT/dt < 10^{-3} K s⁻¹.

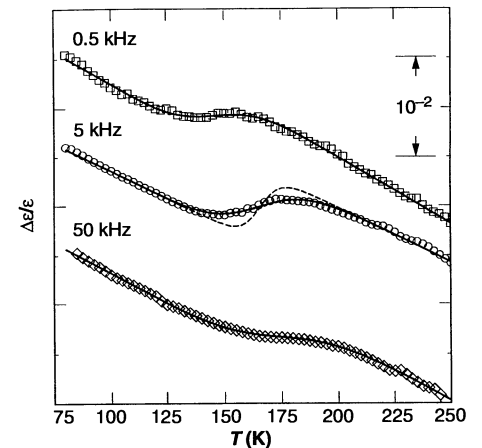


Fig. 2. Expanded view of the dielectric permittivity change $\Delta\epsilon/\epsilon$ for sample S_1 at three frequencies. The dashed line through the 5-kHz data represents a Debye relaxational response for a single activation energy. The solid lines at the three frequencies represent a fit for a Gaussian distribution of activation energies with fixed prefactor and variable mean energy, width, and a background that is linear in temperature. The 50-kHz fit was obtained with a fixed width $W = 40$ meV because of the limited temperature region above the relaxation and below the orientational phase transition. The data are offset vertically for clarity.

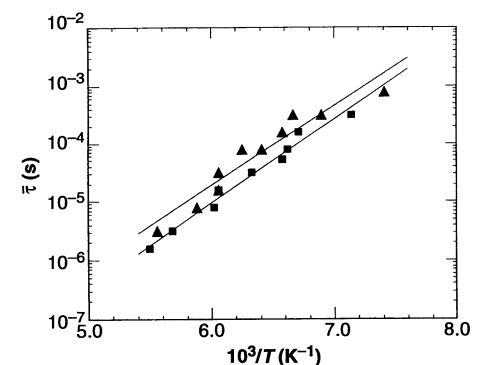


Fig. 3. Mean dipolar relaxation time $\bar{\tau}$ versus $1/T$. The data were obtained by setting $\bar{\tau}^{-1} = \omega$ at the midpoint of the knee (see Fig. 2), where ω is the measurement frequency. The lines are fits to an Arrhenius temperature dependence given by Eq. 3. The triangles represent sample S_1 , and the squares represent sample S_2 .

G. B. Alers and B. Golding, Department of Physics and Astronomy and the Center for Fundamental Materials Research, Michigan State University, East Lansing, MI 48824.

A. R. Kortan, R. C. Haddon, F. A. Theil, AT&T Bell Laboratories, Murray Hill, NJ 07974.

*To whom correspondence should be addressed.

This width is smaller than reported earlier on similar samples (10), which may reflect the care taken here in mounting the soft crystals so as to minimize thermal expansion-induced strains. We observe some evidence of transition broadening on the low-temperature side, as shown in the inset. Nevertheless, at least 70% of the crystal transforms over a 0.5 K temperature interval.

Below T_c we observe a contribution to the dielectric function that can be described by relaxational dynamics. At 10 kHz this process gives rise to the knee in $\Delta\epsilon/\epsilon$ and the broad maximum in σ seen in Fig. 1 near 165 K. Figure 2 shows a detailed view of $\Delta\epsilon/\epsilon(\omega, T)$ at three frequencies. As the frequency increases, the knee in $\Delta\epsilon/\epsilon$ moves to higher temperature, suggestive of a strongly temperature-dependent relaxation time. Nevertheless, the data cannot be described by a unique value of $\tau(T)$. To demonstrate this, we show in Fig. 2 (dashed line) the response of a single Debye relaxation time. To explain the data, we shall assume that a Gaussian distribution (20) of activation energies exists, centered at E_0 with width W such that

$$\Delta\epsilon(T) =$$

$$\frac{1}{W\sqrt{\pi}} \int_0^\infty dE e^{-\left(\frac{E-E_0}{W}\right)^2} \Delta\epsilon_1(E, T) \quad (1)$$

$$\Delta\epsilon_1(E, T) = \frac{A}{1 + (\omega\tau)^2} \quad (2)$$

$$\tau = \tau_0 \exp\left(\frac{E}{k_B T}\right) \quad (3)$$

where A and τ_0 are constants and ω is the measurement frequency. Equation 2 represents the response of a single Debye relaxation, and Eq. 3 indicates that the transition times are thermally activated. We perform a least squares fit of Eq. 1 to the data, allowing for a background term that is linear in T . The fits are shown in Fig. 2 by the solid lines and yield a width W of 41 ± 6 meV and a barrier energy of 270 ± 10 meV. The uncertainty indicates differences in fits for eight sets of data at all frequencies measured for S_1 . The main contribution to the uncertainty results from an overly simple background function that deviates from linearity as T_c is approached. This form of the relaxation function is adequate to describe our data at the present accuracy (21). Irrespective of the specific distribution function, we conclude that the broad distribution of potential energy barriers is clear evidence for some form of disorder.

The activation energy can be obtained either from our fits of Eq. 1 or through the temperature dependence of the mean $\bar{\tau}$, assuming that $\bar{\tau}^{-1} = \omega$ at the midpoint of the knee in Fig. 2. Figure 3 shows $\bar{\tau}(T)$ as a function of $1/T$ for dielectric measurements

on both samples over nearly three decades of frequency. The mean relaxation time $\bar{\tau}$ is well described by an Arrhenius law, Eq. 3. Results for both samples are shown, with $E_0 = 270 \pm 10$ meV and $\tau_0 = 1 \times 10^{-13}$ s for S_1 and $E_0 = 280 \pm 10$ meV and $\tau_0 = 2 \times 10^{-14}$ s for S_2 . These parameters are close to results derived from ^{13}C NMR motional narrowing experiments for which $E_0 = 250$ meV and $\tau_0 = 3 \times 10^{-14}$ s (6). More recent experiments on elastic properties (10) and on thermal conductivity (12) are also in agreement with these numbers.

The observation of a dielectric relaxation process that requires a permanent electric dipole seems quite surprising for a system that has a center of symmetry at the molecular and crystallographic levels. Nevertheless, we argue that the disorder responsible for the required distribution of barrier energies for orientational hopping breaks the local inversion symmetry and allows a permanent dipole to exist. The currently accepted picture of the low-temperature, orientationally ordered phase involves four simple cubic sublattices differentiated by rotations of C_{60} about the four distinct $\langle 111 \rangle$ axes centered on the hexagon faces (3, 9). This model pairs pentagon faces with hexagon edges for all nearest neighbor C_{60} molecules. In this structure both the molecule and the lattice have inversion symmetry that does not allow a permanent dipole moment on the C_{60} (22). Various forms of disorder can break the inversion symmetry and induce a permanent electric dipole moment on the molecule. A single isolated point defect will not have a disorder-induced dipole moment because the surrounding lattice still has inversion symmetry. A dipole moment may, however, be induced on the nearest neighbors of a misoriented C_{60} as a result of the broken inversion symmetry at the nearest neighbor lattice site. In order to contribute to the susceptibility, the dipole of the neighbor must reorient in response to the electric field. Reorientation of a neighbor of an existing misoriented C_{60} introduces a second orientational defect, and therefore we require a two-defect model to generate the dipolar response. The rotation of the C_{60} must involve two inequivalent configurations such that the dipole changes with the molecular reorientation. Another type of point defect, such as a vacancy, C_{70} , or foreign impurity, could induce a dipole moment on the neighbors, but rotation of a neighboring C_{60} molecule would not significantly change this dipole (assuming that the effect of a neighbor's orientation is small relative to the strain field of the defect). Therefore, the simplest picture for a dipolar relaxation in solid C_{60} requires at least two nearest neighbor orientational defects and a rotation that changes the

induced dipole moment of the two defects.

It is also possible, but less likely, that extrinsic dipolar chemical impurities are responsible for the relaxation. A net moment could exist on a chemical variant of C_{60} but, judging from the difficulty in synthesizing such species (23), this seems somewhat unlikely. Another possibility is that dipolar impurities are incorporated into the crystal's interstices subsequent to crystal growth. There are several arguments to counter this idea. First, the dielectric relaxation strength is remarkably similar for both samples, $\Delta\epsilon/\epsilon = (5.8 \pm 1) \times 10^{-3}$ for S_1 and $(5.3 \pm 1) \times 10^{-3}$ for S_2 . Yet, the two crystals had different thermal histories and different exposures to atmospheric contaminants, and their electrical conductivities differ by an order of magnitude. This finding suggests that the contaminants present do not affect the orientational relaxation response. Second, the diffusion of atmospheric gases, for example, O_2 , H_2O , and so forth, into single crystals is relatively slow and would represent a small contaminated volume. Finally, the orientational dynamics as sensed by NMR spectroscopy, phonons, and dielectric response are so similar that the evidence points to an intrinsic phenomenon.

It is possible to estimate the magnitude of the permanent electric dipole moment on the C_{60} . If we assume a simple Debye model for a permanent dipole that can freely orient (taking an orientational average of one-third as an upper limit), then the polar contribution to ϵ is given by $A = (4\pi n p^2 / 3k_B T)$, where A corresponds to the amplitude given in Eq. 2, n is the density of dipoles, and p is the permanent dipole moment. If we further assume that every molecule has the same disorder-induced dipole such that n is the molecular density, then the observed relaxation strength $\Delta\epsilon/\epsilon = 5 \times 10^{-3}$ corresponds to a permanent dipole moment $p = e r_0 = 2 \times 10^{-19}$ esu/molecule (where e is the electronic charge). Taking $r_0 = 7 \text{ \AA}$, the diameter of a C_{60} molecule, this would correspond to a charge asymmetry of $6 \times 10^{-3} e$ per molecule. On the other hand, if the number of entities carrying a dipole is smaller, we could expect a larger dipole. Because it is unlikely that the C_{60} dipole moment would be greater than $\sim 5 \times 10^{-18}$ esu, a typical value for highly polar molecules, then there must be a relative concentration of dipolar $C_{60} > 10^{-3}$.

The fraction of molecules with a permanent dipole moment depends on the mechanism for the disorder. David *et al.* (11) fit neutron diffraction data with a model that allowed two possible orientations of the C_{60} differentiated by a 60° rotation about a threefold axis. The fraction of the second orientation was 18% at 90 K and increased

further with T . This degree of disorder gives, on average, at least two nearest neighbors occupying a misoriented configuration. Our results are consistent with this model. Any fraction of orientationally disordered C_{60} molecules greater than 1/12 would be sufficient to induce a dipole on essentially all molecules. Recent calculations (4) have shown that this rotation about a threefold axis should be separated by a 300-meV barrier, which is also consistent with our results. For completeness, we note that the disorder could also originate at nonorientationally induced crystallographic defects such as domain boundaries, stacking faults, or twins. The crystal would have to be highly defective to have at least 10^{-3} of its molecules at disordered interfaces.

Finally, we can address the question of "glassy" behavior in crystalline C_{60} . Our results show a high degree of static orientational disorder and invite a comparison with the well-studied orientational glass $KBr_{1-x}(CN)_x$. The width of the barrier height distribution in $KBr_{0.5}(CN)_{0.5}$ is 30 meV (20), quite comparable to the 40-meV width for C_{60} . But in $KBr_{0.5}(CN)_{0.5}$ the mean barrier energy E_0 is 60 meV such that the fractional width is $W/E_0 \approx 0.5$, whereas in C_{60} the mean barrier energy is 270 meV and the fractional width is $W/E_0 \approx 0.15$. Therefore, if the fractional width is generated by intermolecular interactions, then they must be less important in C_{60} relative to glassy $KBr_{0.5}(CN)_{0.5}$. We also note that $KBr_{1-x}(CN)_x$ has no glassy phase for $x > 0.7$ where $W/E_0 < 0.4$ (20). Another signature of glassy behavior would be deviations from Arrhenius behavior resulting in a Vogel-Fulcher law near a glass transition. Figure 3 shows no deviations from Arrhenius behavior for the temperature range 130 K $< T < 190$ K. In addition, thermal conductivity measurements (12), which extended to 85 K, have found $E_0 = 240 \pm 30$ meV, close to our higher temperature results. The consistency of these different measurements over a large spread in time scales would imply that Arrhenius behavior persists to 85 K (24). Therefore, whether C_{60} has quenched disorder or a low-temperature glassy phase appears to be an open question for the moment.

Our results indicate that cubic crystals of solid C_{60} couple to low-frequency electric fields in a way that reflects the orientational dynamics of the C_{60} molecules. There appears to be a relatively large amount of structural disorder, most likely originating in the imperfect orientational alignment of adjacent molecules. The disorder creates a distribution of potential barriers for molecular reorientation and breaks the local symmetry sufficiently to allow a permanent electric dipole to exist on a C_{60} molecule.

REFERENCES AND NOTES

- H. W. Kroto, J. R. Heath, S. C. O'Brien, R. F. Curl, R. E. Smalley, *Nature* **318**, 162 (1985).
- W. Kratschmer, L. D. Lamb, K. Fostiropoulos, D. R. Huffman, *ibid.* **347**, 354 (1990).
- P. A. Heiney *et al.*, *Phys. Rev. Lett.* **66**, 2911 (1991); R. Sachidanandam and A. B. Harris, *ibid.* **67**, 1467 (1991).
- J. P. Lu, X.-P. Li, R. Martin, *ibid.* **68**, 1551 (1992).
- O. Gunnarsson, S. Satpathy, O. Jepsen, O. K. Andersen, *ibid.* **67**, 3002 (1991).
- R. Tycko *et al.*, *ibid.*, p. 1886.
- D. A. Neumann *et al.*, *ibid.*, p. 3808.
- R. D. Johnson, C. S. Yannoni, H. C. Dorn, J. R. Salem, D. S. Bethune, *Science* **255**, 1235 (1992).
- W. I. F. David *et al.*, *Nature* **353**, 147 (1991).
- X. D. Shi *et al.*, *Phys. Rev. Lett.* **68**, 827 (1992).
- W. I. F. David *et al.*, *Europhysics Lett.* **18**, 219 (1992).
- R. C. Yu, N. Tea, M. B. Salamon, D. Lorents, R. Malhotra, *Phys. Rev. Lett.* **68**, 2050 (1992).
- W. P. Beyermann *et al.*, *ibid.*, p. 2046.
- M. P. Gelfand and J. P. Lu, *ibid.*, p. 1050.
- Toluene was used in the extraction from the soot, and C_{60} was separated by column chromatography. Sample purity was verified by high-performance liquid chromatography, which found no trace of other fullerenes at a level of a fraction of a percent. The C_{60} powder was then loaded in a quartz tube sealed in a vacuum (10^{-6} torr) and the end of the tube heated to 600°C. High-quality single crystals grew at 350° to 300°C over a period of a few weeks. See R. M. Fleming *et al.*, *Mater. Res. Soc. Symp. Proc.* **206**, 691 (1991).
- A. F. Hebard, R. C. Haddon, R. M. Fleming, A. R. Kortan, *Appl. Phys. Lett.* **59**, 2109 (1991).
- Y. Saito *et al.*, *Chem. Phys. Lett.* **189**, 236 (1992).
- S. Saito and A. Oshiyama, *Phys. Rev. Lett.* **66**, 2637 (1991); W. Y. Ching *et al.*, *ibid.* **67**, 2045 (1991).
- P. A. Heiney *et al.*, *Phys. Rev. B* **45**, 4544 (1992).
- R. M. Ernst *et al.*, *ibid.* **38**, 6246 (1988); F. Luty and J. Ortiz-Lopez, *Phys. Rev. Lett.* **50**, 1289 (1983).
- Uncertainties in the background make a quantitative discrimination among different relaxation functions difficult. For example, a stretched exponential relaxation function yielded a reasonable description of the data.
- The same Pa3 symmetry of C_{60} is also found in solid H_2 and N_2 with no permanent dipole moment. Intermolecular interactions between quadrupolar H_2 and N_2 can induce a dipolar response for certain phonon modes. See O. Schnepp, *J. Chem. Phys.* **46**, 3983 (1967); J. Van Kranendonk, *Solid Hydrogen* (Plenum, New York, 1983), pp. 114–128.
- T. Suzuki, Q. Li, K. C. Khemani, F. Wudl, O. Almarsson, *Science* **254**, 1186 (1991).
- In $KBr_{0.5}(CN)_{0.5}$, a transition to a quadrupolar glass phase occurs near 80 K followed by electric dipolar freezing near 50 K. No anomalies in the dielectric response have been seen at the quadrupolar glass transition. In C_{60} , it is possible that there is an order parameter to which strain and electric field do not couple.
- We acknowledge helpful conversations with N. O. Birge, S. D. Mahanti, and M. F. Thorpe.

28 April 1992; accepted 28 May 1992

High-Pressure Brillouin Studies and Elastic Properties of Single-Crystal H_2S Grown in a Diamond Cell

H. Shimizu and S. Sasaki

High-pressure Brillouin spectra of crystalline hydrogen sulfide (H_2S) have been measured at up to 7 gigapascals at room temperature. The best fit of the angular dependence of Brillouin acoustic velocities between experimental values and calculations based on Every's expression for elastic waves of an arbitrary direction yielded the orientation of an H_2S cubic crystal grown in the diamond-anvil high-pressure cell. In situ determinations of sound velocities, as a function of pressure, could be made for any direction, the refractive index, the density, and the elastic constants. This method provides a means for the systematic study of elastic properties and phase transitions of condensed gases under ultrahigh pressures.

High-pressure Brillouin scattering is an ideal probe for measuring the sound velocity (v), the refractive index (n) and the elastic constant (C_{ij}) as a function of pressure, and the equation of state (EOS) (1–4). When a typical diamond-anvil high-pressure cell (DAC) is used, the probed direction for the wave vector (q) of the acoustic phonon propagating in a crystal is considerably limited (1, 4, 5): only one or two directions of q parallel to the diamond culet faces for a scattering geometry of 90° and only one direction of q perpendicular to the diamond faces for the backscattering

geometry can be used (1, 4, 6–8). It is then necessary to determine accurately the axis orientation of the grown crystal, because the sound velocity is sensitively dependent on the direction of q for the probed acoustic phonon, but this has been difficult. Lee *et al.* (7) overcame the above problem by the additional use of x-ray diffraction measurements. They determined the axis orientation of a single crystal of orthorhombic hydrogen-bonded HF and measured the high-pressure Brillouin spectra of oriented HF crystals at the near-forward scattering geometry, which yielded the sound velocities as a function of pressure, and the values of five elastic constants divided by the density (C_{ij}/ρ) at a pressure of 2.54 GPa.

Department of Electronics, Gifu University, 1-1 Yanagido, Gifu 501-11, Japan.